Variability of Chain Transfer to Monomer Step in Olefin Polymerization

Giovanni Talarico[†] and Peter H. M. Budzelaar*[,‡]

Dipartimento di Chimica Paolo Corradini, Università di Napoli Federico II, Via Cintia, 80126 Napoli, Italy, and Department of Chemistry, University of Manitoba, Winnipeg MB R3T 2N2, Canada

Received April 7, 2008

Computational studies of a variety of polymerization catalyst models have revealed an unexpected fluidity in chain termination mechanisms. For many early transition metal olefin polymerization catalysts two distinct transition states exist for β-hydrogen transfer to monomer, which differ mainly in the M−H distance and CMC angle. The transition state for the "classical" (BHT_A) path resembles a metal hydride−bis(olefin) complex, whereas the alternative BHT_B path involves direct transfer of an alkyl β-hydrogen to a coordinated olefin without any metal−hydride interaction. The two transition states are separated by a second-order saddle point that is just a few kcal/mol above the highest of the two transition states, indicating a flat potential-energy surface between the two paths. Of the group IV metals, Zr (in contrast to Ti and Hf) appears to have an intrinsic preference for the "classical" BHT_A path. *Increasing* the amount of space around the metal (e.g., in lanthanocenes) changes BHT_A into a two-step path (BHT_C), showing two β-hydride elimination transition states around a hydride−bis(olefin) complex local minimum. *Decreasing* the amount of space by using sterically demanding ligands results in a shift toward the "new" BHT_B path. However, β-hydrogen elimination becomes more favorable at the same time, and our results suggest that for most early transition metal catalysts (typically 14-*e* metal alkyls) either BHT_A or β-hydrogen elimination will be the dominant chain-transfer pathway, whereas BHT_B may be relevant for some Hf complexes of intermediate crowding. The BHT_B path is expected to be more important for systems that are less unsaturated (16-*e* transition metal alkyls; 6-*e* main-group metal alkyls) and also for "hetero-olefin" derivatives (alkoxides, amides), where β-hydrogen elimination is strongly endothermic.

Introduction

Metal-catalyzed olefin polymerization is conceptually one of the simplest metal-catalyzed reactions, having just a single elementary step (insertion)[1] and often a resting stage *within* the catalytic cycle (β-agostic alkyl or alkyl−olefin complex). It is also a reaction of tremendous industrial importance and, hence, has been studied in great detail over the last half-century.[2] Remarkably, these studies keep yielding surprises and demonstrate that the conceptual simplicity actually hides an amazing complexity, both in propagation itself and in the various reactions leading to chain termination or catalyst deactivation. In the present paper, we will concentrate on chain termination mechanisms intrinsic to the catalytic species, i.e., mechanisms that do not involve counterions, cocatalysts, or added chain-transfer agents.

One of the most important properties of a polymer is its (average) chain length. For metal-catalyzed olefin polymerization, the degree of polymerization is determined by the ratio between the rate of propagation and those of all possible chain termination mechanisms. There are very many potential chain termination (CT) reactions; Scheme 1 illustrates the ones considered in the present work. For the more efficient olefin polymerization catalysts, it is generally accepted that—in the absence of added chain-transfer agents—the most important ones are β-hydrogen elimination (BHE) and β-hydrogen transfer to monomer (BHT).

BHE is a very "standard" organometallic reaction and is a common decomposition route for all kinds of metal alkyls carrying β-hydrogen atoms.[3] It is essentially *dissociative*; if this were the dominant CT mechanism, molecular weights would be proportional to the monomer concentration, which is usually not observed in practice. To explain this discrepancy, *associative* chain-transfer reactions have been proposed.[4–7] The first computational studies of β-hydrogen transfer were published in 1995

* Corresponding author. E-mail: budzelaa@cc.umanitoba.ca.
[†] Università di Napoli Federico II.
[‡] University of Manitoba.

(1) This depends on the level of detail with which one draws the cycle. Counterion displacement, breaking of an agostic interaction, and olefin capture could all be considered separate elementary steps.

(2) Recent reviews for heterogeneous Ziegler−Natta catalysts, see e.g.: (a) Kashiwa, N. *J. Polym. Sci. A: Polym. Chem.* **2004**, *42*, 1. (b) Mülhaupt, R. *Macromol. Chem. Phys.* **2003**, *204*, 289. For metallocene catalysts, see e.g.: (c) Resconi, L.; Cavallo, L.; Fait, A.; Piemontesi, F. *Chem. Rev.* **2000**, *100*, 1253. (d) Brintzinger, H.-H.; Fischer, D.; Mülhaupt, R.; Rieger, B.; Waymouth, R. M. *Angew. Chem., Int. Ed.* **1995**, *34*, 1143. For late transition metal, see e.g.: (e) Ittel, S. D.; Johnson, L. K.; Brookhart, M. *Chem. Rev.* **2000**, *100*, 1169. For non-metallocene catalysts, see e.g.: (f) Gibson, V. C.; Spitzmesser, S. K. *Chem. Rev.* **2003**, *103*, 283.

(3) See e.g.: Crabtree, R. H. *The Organometallic Chemistry of the Transition Metals*, 4th ed.; Wiley: Hoboken, N.J., 2005; pp 55 and 191, and references therein.

(4) (a) Zakharov, V. A.; Bukatov, G. D.; Yermakov, Y. I. *Adv. Polym. Sci.* **1983**, *51*, 61. (b) Pino, P.; Rotzinger, B.; Van Achenbach, E. *Makromol. Chem. Suppl.* **1985**, *25*, 461. (c) Kashiwa, N.; Yoshitake, J. *Polym. Bull.* **1984**, *11*, 479. (d) Tsutsui, T.; Mizuno, A.; Kashiwa, N. *Polymer* **1989**, *30*, 428. (e) Boor, J., Jr. *Ziegler-Natta Catalysts and Polymerization*; Academic Press: New York, 1979; pp 258−259, and references therein.

(5) Woo, T. K.; Fan, L.; Ziegler, T. *Organometallics* **1994**, *13*, 2252.

(6) Yang, X.; Stern, C. L.; Marks, T. J. *J. Am. Chem. Soc.* **1994**, *116*, 10015.

(7) Stehling, U.; Diebold, J.; Kirsten, R.; Röll, W.; Brintzinger, H.-H.; Jüngling, S.; Mülhaupt, R.; Langhauser, F. *Organometallics* **1994**, *13*, 964.

10.1021/om800313n CCC: $40.75
Publication on Web 07/23/2008

Scheme 1. Main Chain-Transfer Paths for Olefin Polymerization: β-Hydrogen Elimination (BHE), "Classical" β-Hydrogen Transfer (BHT_A), "New" Transfer (BHT_B), and True Associative Displacement (BHT_C)

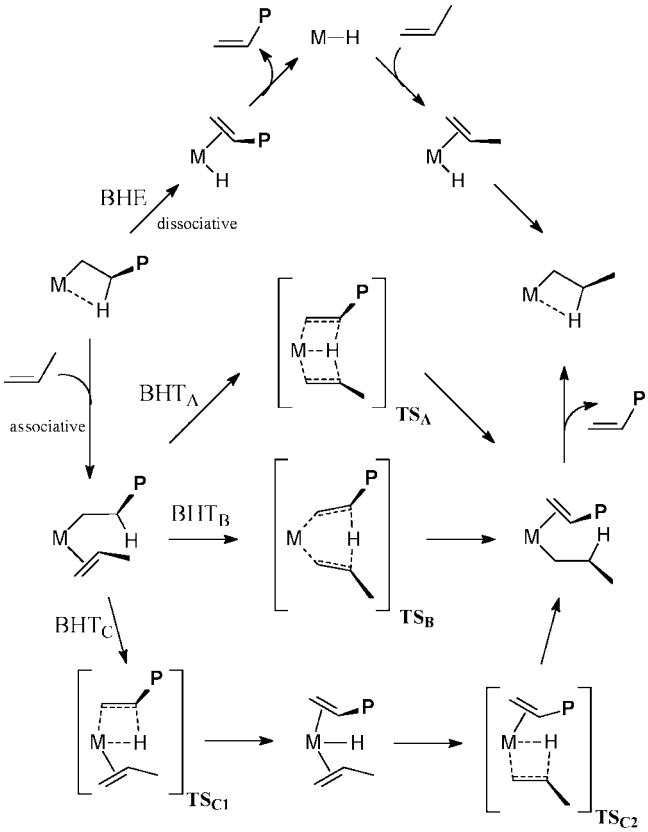

by the group of Ziegler.[8] They showed an *associative* mechanism passing through a transition state (TS_A) that resembles a metal hydride−bis(olefin) complex. A large number of computational studies have confirmed the existence of this kind of transition state for many different catalytic species.[9]

The geometry of the TS has important implications. It has a large CMC angle and therefore requires much more space at the metal than propagation. This has led to "ligand design" strategies where space around the metal is restricted, leading to suppression of BHT and higher molecular weights.[8,9] Such strategies cannot be taken to extremes, since for very crowded systems the dissociative BHE path (or even β-methyl elimination) becomes more accessible. Nevertheless, this design principle has been surprisingly successful in the design of modern catalysts, both metallocene[9a] and nonmetallocene based.[9b]

About 10 years ago we reported on chain-transfer mechanisms for the main-group metal aluminum.[10] The BHT transition state calculated for that metal looks very different from the one mentioned above and features a large M−H distance. There is no direct metal−hydride interaction, and the reaction is best considered as an organometallic equivalent of an organic ene reaction.[10b] This has led us to investigate whether such a TS could also exist (perhaps independently) for transition-metal polymerization catalysts. In an earlier communication, we confirmed that this is indeed the case.[11] In the remainder of this paper, we will indicate the "classical" path as BHT_A and the "new" path as BHT_B. Interestingly, the geometry of the associative TS proposed in 1994 by Brintzinger[7] resembles this alternative BHT_B TS (for simplicity TS_B) in that it was drawn without direct metal−hydride interaction, but on the other hand shows the wide CZrC angle characteristic of the BHT_A TS (in the following, TS_A) first studied by the group of Ziegler.[8]

In itself, the BHT_B path is not new. A TS_B-like geometry has been calculated as the preferred path for β-hydrogen transfer as a diiminepyridine cobalt(I) system[12] (which does *not* polymerize), while for an α-diimine palladium(II) system such a TS was predicted to exist but to be much too high in energy to be relevant to polymerization.[13] One of our more remarkable findings was that, at least for metallocene-like systems, the BHT_A and BHT_B paths are separated by only a small energy "barrier" (typically less than 5 kcal/mol), so that small changes to the system can lead to (dis)appearance of one of the two reaction paths.

In the present work, we demonstrate that there is even more "fluidity" in chain termination mechanisms and that there is in fact a near-continuum not only between BHT_A and BHT_B but even between BHE, BHT_A, and a situation with a stable hydride−bis(olefin) *intermediate* (BHT_C, also illustrated in Scheme 1), as found in previous computational studies on certain late-transition-metal systems.[13,14] We explore the dependence of the situation on the choice of metal, ligand, olefin, and computational methods. In order to assess the relevance of the BHT_B path for real polymerization catalysts, we attempt—for the first time—to put all relevant reactions (propagation, BHT_A, BHT_B, BHE) on a common energy scale. Finally, our wide-ranging exploration allows us to rationalize the preferences of different systems for different chain-transfer mechanisms.

Methods

The systems investigated systematically are shown in Scheme 2. For all of these, we studied the various reactions of the LM(^{t}Bu) species with propene, as a model of chain growth/termination in propene polymerization. In addition, several Co, Pd, and Al systems were investigated, as described later in this paper. All geometries were fully optimized as minima, transition states, or second-order

(8) (a) Fan, L.; Harrison, D.; Deng, L.; Woo, T. K.; Swerhone, D.; Ziegler, T. *Can. J. Chem.* **1995**, *73*, 989. (b) Lohrenz, J. C. W.; Woo, T. K.; Fan, L.; Ziegler, T. *J. Organomet. Chem.* **1995**, *497*, 91. (c) Lohrenz, J. C. W.; Woo, T. K.; Ziegler, T. *J. Am. Chem. Soc.* **1995**, *117*, 12793.

(9) See e.g.: (a) Rappé, A. K.; Skiff, W. M.; Casewit, C. J. *Chem. Rev.* **2000**, *100*, 1435, and references therein for metallocene systems. (b) Busico, V.; Cipullo, R.; Pellecchia, R.; Ronca, S.; Roviello, G. *Proc. Natl. Acad. Sci. U.S.A.* **2006**, *103*, 15321. (c) Talarico, G.; Busico, V.; Cavallo, L. *Organometallics* **2004**, *23*, 5989, and references therein for post-metallocene systems.

(10) (a) Talarico, G.; Budzelaar, P. H. M.; Gal, A. W. *J. Comput. Chem.* **2000**, *21*, 398. (b) Budzelaar, P. H. M.; Talarico, G. *Struct. Bonding (Berlin)* **2003**, *105*, 141, and references therein.

(11) Talarico, G.; Budzelaar, P. H. M. *J. Am. Chem. Soc.* **2006**, *128*, 4524.

(12) Tellmann, K. P.; Humphries, M. J.; Rzepa, H. S.; Gibson, V. C. *Organometallics* **2004**, *23*, 5503.

(13) (a) Musaev, D. G.; Svensson, M.; Morokuma, K.; Strömberg, S.; Zetterberg, K.; Siegbahn, P. E. M. *Organometallics* **1997**, *16*, 1933. (b) Musaev, D. G.; Froese, R. D. J.; Morokuma, K. *Organometallics* **1998**, *17*, 1850. (c) Musaev, D. G.; Morokuma, K. *Top. Catal.* **1999**, *7*, 107. (d) Froese, R. D. J.; Musaev, D. G.; Morokuma, K. *J. Am. Chem. Soc.* **1998**, *120*, 1581.

(14) (a) Woo, T. K.; Blöchl, P. E.; Ziegler, T. *J. Phys. Chem. A* **2000**, *104*, 121. (b) Woo, T. K.; Ziegler, T. *J. Organomet. Chem.* **1999**, *591*, 204. (c) Deng, L.; Woo, T. K.; Cavallo, L.; Margl, P. M.; Ziegler, T. *J. Am. Chem. Soc.* **1997**, *119*, 6177. (d) Deng, L.; Margl, P.; Ziegler, T. *J. Am. Chem. Soc.* **1997**, *119*, 1094. (e) Michalak, A.; Ziegler, T. *Organometallics* **1999**, *18*, 3998.

(15) (a) Lee, C.; Yang, W.; Parr, R. G. *Phys. Rev. B* **1988**, *37*, 785. (b) Becke, A. D. *J. Chem. Phys.* **1993**, *98*, 1372. (c) Becke, A. D. *J. Chem. Phys.* **1993**, *98*, 5648.

(16) (a) Becke, A. D. *Phys. Rev. A* **1988**, *38*, 3098. (b) Perdew, J. P. *Phys. Rev. B* **1986**, *33*, 8822.

Scheme 2. Systems Studied Systematically; M = Ti^{IV}, Zr^{IV}, or Hf^{IV}[a]

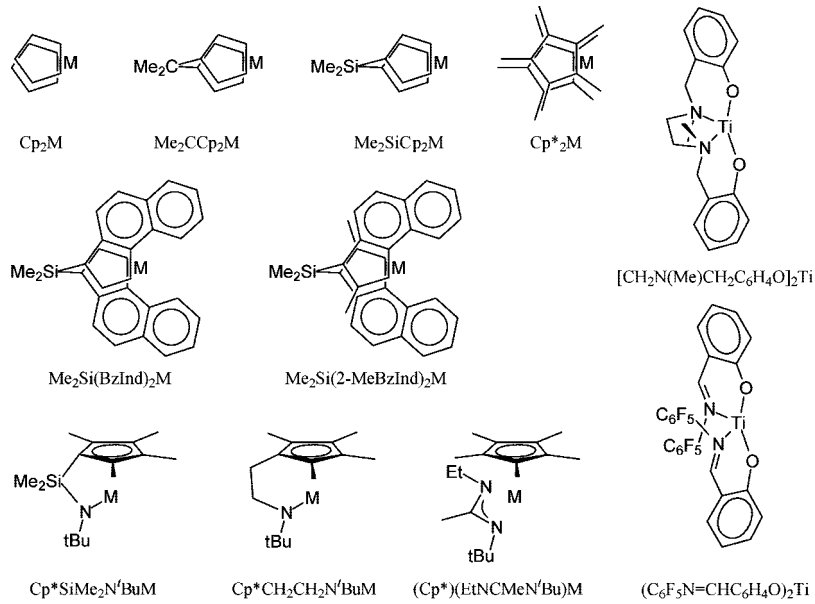

[a] In addition, Cp_2 complexes were studied for Sc^{III}, Y^{III}, La^{III}, and Lu^{III}, and Me_2SiCp_2 complexes for Sc^{III} and Y^{III}.

saddle points using the B3LYP[15] or BP86[16] functionals, in combination with the SVP[17] basis set (LANL2DZ basis and pseudopotential[18] at second- and third-row transition metals) with the Gaussian03 program.[19] For optimization of some transition states and of all second-order saddle points we used our own external optimizer[20] in combination with Gaussian03. Stationary points were characterized using vibrational analyses, and these analyses were also used to calculate zero-point energies and thermal (enthalpy and entropy) corrections (298.15 K, 1 bar). Improved electronic energies were obtained from single-point calculations using a TZVP basis set[21] (SDD basis and pseudopotential[22] at the metal; for Hf, an f function with exponent 0.5 was added).[23] In the remainder of this paper, we will mostly use ΔH^0_{0K}, calculated from the TZVP electronic energy (at SVP geometry) combined with the SVP-level ZPE corrections. For comparison with experiment, however, we will use $\Delta G^0_{298.15K}$, obtained from the TZVP electronic energies and the SVP-level enthalpy and entropy corrections. For a selected set of ligands, solvation corrections (CPCM model,[24] toluene) were explored at the B3LYP/TZVP level.

In this work, we are also comparing reactions at Lu and La. Since the LANL2DZ basis is not available for Lu, geometries for Lu were optimized using the Stuttgart MWB-60 large-core ECP and basis set,[25] and the corresponding La geometries were reoptimized using the MWB-46 large-core ECP and basis set;[22a,25] single-point energies for both were then calculated using the MWB-28 small-core ECP[26] and extended basis set[27] for both metals (TZVP on all other atoms). Total energies, corrections, and geometries are provided in the Supporting Information.

Scheme 3. Competing Transition States for BHT

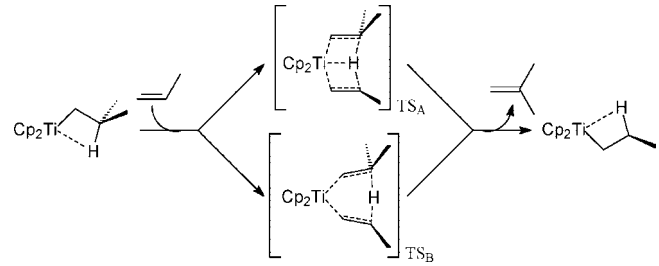

Results and Discussion

Coexistence of BHT_A and BHT_B Paths. We will start with a typical model for chain transfer in metal-catalyzed propene polymerization, as shown in Scheme 3. It uses a simple Cp_2Ti fragment as a model for a metallocene fragment (more realistic ligands will be discussed later) and an isobutyl group as model for a growing polymeryl chain.

The two transition states TS_A and TS_B were located without any problems, and both exhibit the expected single imaginary frequency corresponding to movement of the hydrogen atom. Figure 1(A and C) shows the geometries of these two transition states, and the Supporting Information (SI) contains movies illustrating imaginary normal modes. Several other relevant stationary points (olefin insertion TS, second-order saddle point (SOSP) connecting TS_A and TS_B, species on the BHE path) are also included for comparison.

Comparison of the geometries of TS_B and TS_{ins} shows that they require comparable amounts of space around the metal,

(17) Schäfer, A.; Horn, H.; Ahlrichs, R. *J. Chem. Phys.* **1992**, *97*, 2571.
(18) (a) Dunning., T. H., Jr.; Hay, P. J. In *Modern Theoretical Chemistry*; Schaefer, H. F., III., Ed.; Vol. 3, Plenum: New York, 1976, pp 1−28. (b) Hay, P. J.; Wadt, W. R. *J. Chem. Phys.* **1985**, *82*, 270. (c) Wadt, W. R.; Hay, P. J. *J. Chem. Phys.* **1985**, *82*, 284. (d) Hay, P. J.; Wadt, W. R. *J. Chem. Phys.* **1985**, *82*, 299.
(19) Frisch, M. J.; et al. *Gaussian 03*, Revision C.02; Gaussian, Inc.: Wallingford, CT, 2004; for a complete citation, see the Supporting Information.
(20) Budzelaar, P. H. M. *J. Comput. Chem.* **2007**, *28*, 2226.
(21) Schaefer, A.; Huber, C.; Ahlrichs, R. *J. Chem. Phys.* **1994**, *100*, 5829.
(22) (a) Dolg, M.; Stoll, H.; Preuss, H. *Theor. Chim. Acta* **1993**, *85*, 441. (b) Bergner, A.; Dolg, M.; Kuechle, W.; Stoll, H.; Preuss, H. *Mol. Phys.* **1993**, *80*, 1431.
(23) Re-optimization at the B3LYP/TZVP level was tested for a few systems and resulted in negligible changes in energy and geometry.
(24) (a) Barone, V.; Cossi, M. *J. Phys. Chem. A* **1998**, *102*, 1995. (b) Cossi, M.; Rega, N.; Scalmani, G.; Barone, V. *J. Comput. Chem.* **2003**, *24*, 669.
(25) Dolg, M.; Stoll, H.; Savin, A.; Preuss, H. *Theor. Chim. Acta* **1989**, *75*, 173.
(26) Cao, X.; Dolg, M. *J. Chem. Phys.* **2001**, *115*, 7348.
(27) Cao, X.; Dolg, M. *J. Mol. Struct. (THEOCHEM)* **2002**, *581*, 139.

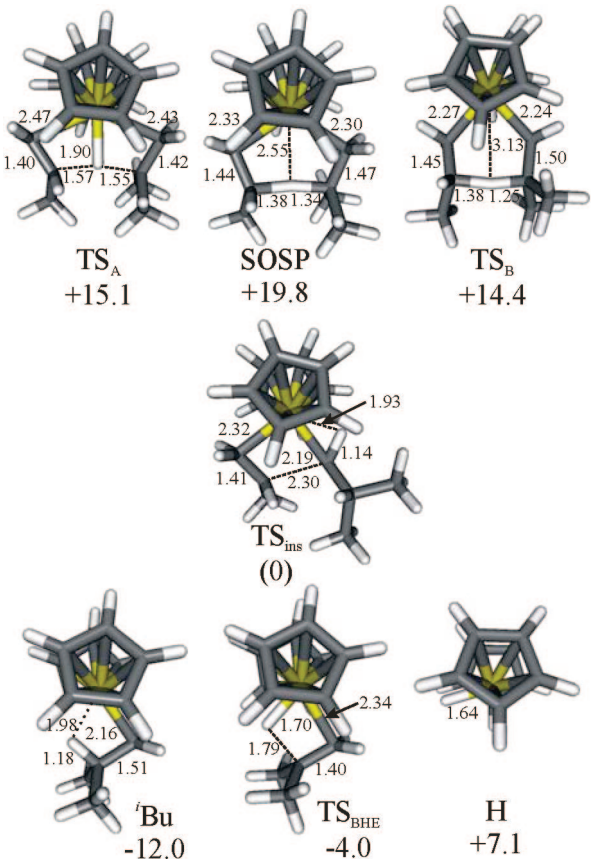

Figure 1. Important stationary points for the $Cp_2Ti^tBu^+$ + propene system. Bond lengths in Å, energies (ΔH^0_{0K} relative to insertion TS) in kcal/mol.

while TS_A requires much more, and of course the metal hydride has by far the smallest space requirements.

It might at first seem strange to have two transition states connecting the same two local minima. In fact, the situation is slightly more complicated, and we will present a more detailed description of the shape of the potential energy surface around the two transition states later in this paper.

Comparison of the geometries of TS_A and TS_B shows that TS_A has smaller C−C distances and larger C···H distances than TS_B and also has an M−H distance only slightly larger than that in the free hydride. This provides justification for regarding TS_A as a transition state for associative olefin exchange at a metal hydride. In contrast, TS_B is a regular six-center TS in which all bonds are made and broken synchronously, as expected for an ene reaction.

Sensitivity to the Method. We have done limited testing of the TS_A/TS_B energy difference with different functionals and basis sets. The effects were found to be minor (1−2 kcal/mol); for further details, see the Supporting Information.

Dependence on the Metal. Metal dependence was explored for group III and IV metallocene models (Table 1). In the series Ti, Zr, Hf, preference for TS_A is strongest for Zr and ca. 5 kcal/mol weaker for *both* Ti and Hf. This somewhat counterintuitive trend is hard to explain. The Ti/Zr difference can be attributed to steric effects, Ti being much smaller than Zr. However, Zr and Hf have virtually the same size, so it seems likely that some electronic factors are important here.

We have not yet come up with a definitive explanation for this difference. Transition state TS_A has significant metal−hydride character, whereas TS_B is simply exchanging one metal−carbon bond for another. One could expect that therefore the TS energies would follow the trend in M−C vs M−H bond strengths.[28] This is indeed found to be the case (see SI), but the Zr/Hf difference of about 2 kcal/mol is too small to explain the trend in Table 1. Since bonds to Hf are generally stronger than those to Zr, one might expect systems to be more rigid, so that the large deformation required to accommodate the space-demanding TS_A geometry would be more difficult to realize. This seems a reasonable argument, but we see no way to unambiguously prove the point.

Table 1. TS_A/TS_B Energy Difference As a Function of Metal

	$\Delta\Delta H^0_{0K}$ (kcal/mol)			
system	Ti	Zr	Hf	
Cp^*_2	−10.0	−1.7	−6.4	
Cp_2	−0.7	7.1	1.6	
Me_2SiCp_2	2.7	9.6	3.9	
$Cp^*SiMe_2N^tBu$	2.7	[a]	3.8	
	Sc	Y	La	Lu
Cp_2	−2.3	3.6	15.2[b]	−1.0
Me_2SiCp_2	−0.2	4.5	[c]	[c]

[a] TS_B could not be located and most likely does not exist. [b] Highest of two TS_C transition states (there is no TS_A); see text. [c] Not calculated.

Extending the exploration to the group III metals, we find that Sc has a TS_A/TS_B energy difference comparable to Ti, and Y has a TS_A/TS_B energy difference comparable to Zr. This is again surprising, since the group III metals are much larger than their group IV counterparts: increased space should have shifted the balance to TS_A. Apparently, the steric effect is counteracted by an electronic effect, which we again are unable to identify.

Interestingly, and unlike for Zr→Hf, the preference for TS_A *increases* if we go from Y to La. In addition, the potential-energy surface (PES) changes qualitatively, now featuring two transition states (TS_{C1}, TS_{C2}) surrounding a hydride−bis(olefin) complex; this is an example of the BHT_C path mentioned in the Introduction (Scheme 1). However, if we now move from La to Lu, the normal single-TS BHT_A profile is restored and the preference shifts back in the direction of TS_B. Apparently, it is the large size of La that causes its deviating behavior; Lu, having nearly the same size as Y, shows the same relation to Y as Hf does to Zr. Figure 2 shows the relevant stationary points on the BHT paths of Cp_2La and Cp_2Lu.

Dependence on the Olefin. This was explored for simple metallocenes by comparing models for propene and ethene polymerization (Table 2). The ethene polymerization model has ethene inserting in an *n*-propyl chain model. Inspection of the results shows that TS_B is 5−6 kcal/mol less favorable (relative to TS_A) for ethene than for propene, which we attribute to the lower steric requirements for reactions involving this small monomer. Electronic factors should go the other way, since the hydrocarbon fragments in TS_A are more "olefin-like" than in Ts_B and methyl groups stabilize C=C bonds.

Dependence on the Ligand Environment. We have covered a wide variety of more or less realistic ligand variations for the group IV metals Ti, Zr, and Hf (Scheme 2). The results are summarized in Table 3. The general trend is that more crowding favors TS_B, while for more open systems TS_A is clearly preferred. For Zr, which already has an intrinsic preference for TS_A, the alternative TS_B entirely ceases to exist for open systems like constrained-geometry catalysts. For the other two metals, the TS_A/TS_B difference can even be used to order the ligands for their effective steric demands. The results suggest that $Me_2Si(2\text{-}MeBzInd)_2$ is comparable to the Cp_2 environment in

(28) Martinho Simões, J. A.; Beauchamp, J. L. *Chem. Rev.* **1990**, *90*, 629.

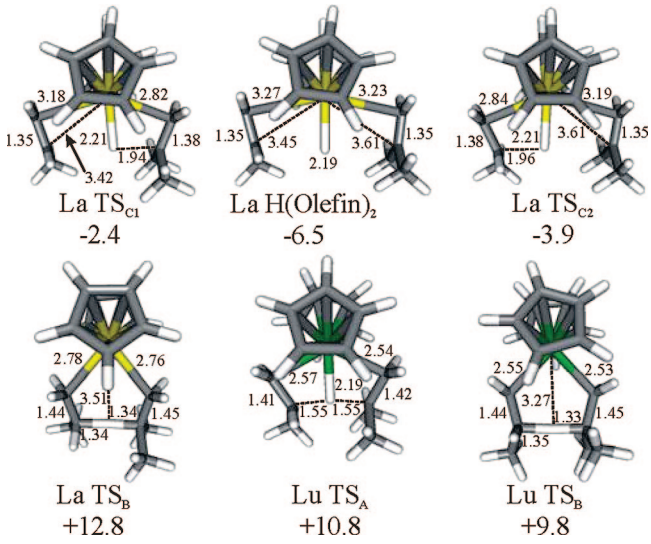

Figure 2. Stationary points for the BHT paths of Cp_2La and Cp_2Lu. Bond lengths in Å, energies (ΔH^0_{0K} relative to insertion TS) in kcal/mol.

Table 2. TS_A/TS_B Energy Difference for Cp_2M Systems As a Function of Olefin

	$\Delta\Delta H^0_{0K}$ (kcal/mol)		
alkyl/olefin	Ti	Zr	Hf
^{i}Bu/propene	−0.7	7.1	1.6
^{n}Pr/ethene	6.2	12.4	6.5

Table 3. TS_A/TS_B Energy Difference As a Function of Ligand Environment

	$\Delta\Delta H^0_{0K}$ (kcal/mol)		
system	Ti	Zr	Hf
(Cp*)(EtNCMeN^{t}Bu)	−10.9	−9.8	−15.4
Cp*$_2$	−10.0	−1.7	−6.4
Cp_2	−0.7	7.1	1.6
$Me_2Si(2\text{-}MeBzInd)_2$	−0.6	5.5	0.2
$Me_2Si(BzInd)_2$	0.5	6.2	0.1
Cp*$CH_2CH_2N^tBu$	1.5	[a]	2.9
Me_2SiCp_2	2.4	9.6	3.9
Cp*$SiMe_2N^tBu$	2.7	[a]	3.8
Me_2CCp_2	4.3	[a]	4.9
$(C_6F_5N{=}CHC_6H_4O)_2$[c]	5.8	[b]	[b]
$[CH_2N(Me)CH_2C_6H_4O]_2$[d]	9.5	[b]	[b]

[a] TS_B could not be located and most likely does not exist. [b] Not calculated. [c] See ref 30.[30] [d] See ref 31.

size: adding a bridge to the Cp_2 system opens it up considerably, but crowding by the substituents compensates for this. The Cp*/acetamidinate environment, reported by Sita,[29] is the bulkiest of all. The two octahedral systems we included, models for phenoxyamine (Kol-type catalysts)[30] and phenoxyimine (FI-type)[31] ligated early-transition-metal complexes, show a much higher preference for TS_A than the metallocene or constrained-geometry catalysts, indicating that they are much less crowded (at least at positions relevant to the BHT transition states).

Shape of the Potential-Energy Surface (PES). As noted before, it seems somewhat unusual to have the same two local minima (the two metal−alkyl−olefin complexes) connected by two different transition states. In fact, we do not know of a similar example in the area of homogeneous catalysis. To investigate this point further, we decided to study the shape of the PES near these minima and transition states in more detail.

Scheme 4. IRC Following from TS_A

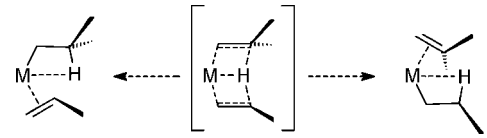

Scheme 5. IRC Following from TS_B

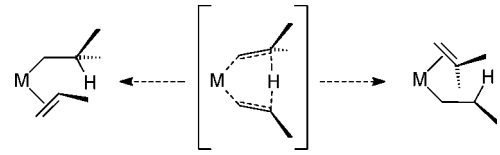

For Cp_2Ti and Cp_2Zr, intrinsic reaction coordinate (IRC)[32] following from the "classical" TS_A led toward "frontside-agostic" (FS) alkyl−olefin complexes (Scheme 4). The PES for movement of the olefins in these structures is extremely shallow, so the IRC calculations did not lead to well-defined minima for these complexes, but the direction of the path was clear enough. In contrast, IRC following from TS_B led to nonagostic alkyl−olefin complexes (Scheme 5). The olefin is more strongly bound here, so the paths actually ended up close to well-defined minima.

Presumably, there would also be transition states connecting the frontside-agostic and nonagostic complexes, but due to the flatness of the PES, we could not locate these. A situation like this, with four local minima connected pairwise by two types of reactions, would be expected to have a second-order saddle point (SOSP) connecting the four transition states (see Scheme 6), and indeed we managed to locate such an SOSP for all cases where both TS_A and TS_B could be located (see Table 4). Figure 1 shows the structure of one such SOSP, and the SI has movies illustrating its two imaginary normal modes.

The height of the SOSP above TS_A and TS_B indicates how well the two reaction paths are separated. A SOSP that is high above both transition states means that small changes to the system (either chemical or changes to computational methods) will not affect the existence of the two paths. In the present case, however, the SOSP is usually only a few kcal/mol above the highest of the transition states it connects, so that a small change could already make, for example, both the SOSP and one transition state disappear, and this is apparently what happens for the more open Zr systems. In the somewhat unusual case of Cp_2La, where the BHT_A path has been replaced by the BHT_C path, the SOSP still exists, although it is only 0.1 kcal/mol above TS_B.

For very crowded systems, on the other hand, olefin complexation becomes so weak that the FS-agostic local minima disappear. In this case, the TS_A and TS_B transition states truly connect the same two local minima. In order to disentangle the

(29) (a) Sita, L. R.; Jayaratne, K. C. *J. Am. Chem. Soc.* **2000**, *122*, 958. (b) Jayaratne, K. C.; Keaton, R. J.; Henningsen, D. A.; Sita, L. R. *J. Am. Chem. Soc.* **2000**, *122*, 10490. (c) Sita, L. R.; Keaton, R. J.; Jayaratne, K. C.; Fettinger, J. C. *J. Am. Chem. Soc.* **2000**, *122*, 12909.

(30) Tshuva, E. Y.; Goldberg, I.; Kol, M. *J. Am. Chem. Soc.* **2000**, *122*, 10706.

(31) For patents on basic and modified FI systems see e.g.:(a) Mitani, M.; Yoshida, Y.; Mohri, J.; Tsuru, K.; Ishii, S.; Kojoh, S.-I.; Matsugi, T.; Saito, J.; Matsukawa, N.; Matsui, S.; Nakano, T.; Tanaka, H.; Kashiwa, N.; Fujita, T. World Pat. Appl. . 01/55231 A1, 2001 (filed in January 2000). (b) Coates, G. W.; Tian, J.; Hustad, P. D. U.S. Patent 6562930, 2003 (filed in September 2001). For a review on FI systems see e.g.:(c) Coates, G. W.; Hustad, P. D.; Reinartz, S. *Angew. Chem., Int. Ed.* **2002**, *41*, 2236. (d) Sakuma, A.; Weiser, M.-S.; Fujita, T. *Polym. J.* **2007**, *39*, 193.

(32) (a) Gonzalez, C.; Schlegel, H. B. *J. Chem. Phys.* **1989**, *90*, 2154. (b) Gonzalez, C.; Schlegel, H. B. *J. Chem. Phys.* **1990**, *94*, 5523.

Scheme 6. Relations between Minima and Transition States (bracketed) on the BHT_A and BHT_B Paths

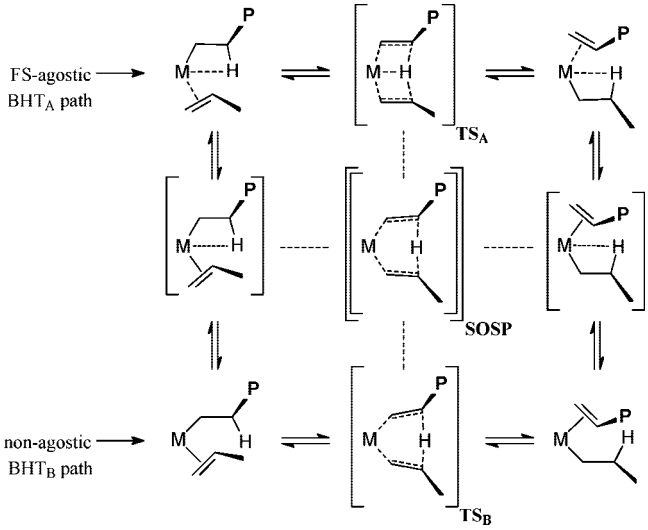

Table 4. SOSP Energies Relative to *Highest* BHT TS

	$\Delta\Delta H^0_{0K}$ (kcal/mol)			intrinsic $\Delta\Delta H^0_{0K}$ (kcal/mol)[a]		
system	Ti	Zr	Hf	Ti	Zr	Hf
(Cp*)(EtNCMeN^{t}Bu)	1.4	2.0	0.01	5.4	5.8	4.1
Cp^*_2	−0.03[d]	2.8	0.5	[d]	3.6	2.8
Cp_2	4.7	1.4	2.8	5.0	4.2	3.6
$Me_2Si(2\text{-}MeBzInd)_2$	2.1	0.1	2.0	2.4	1.8	2.1
$Me_2Si(BzInd)_2$	3.2	0.5	2.2	3.4	2.7	2.7
$Cp^*CH_2CH_2N^tBu$	2.0	[b]	−0.2[d]	2.7	[b]	[d]
Me_2SiCp_2	3.5	0.1	1.4	4.6	2.9	3.0
$Cp^*SiMe_2N^tBu$	1.5	[b]	−0.3[d]	2.7	[b]	[d]
Me_2CCp_2	2.1	[b]	0.7	4.0	[b]	2.6
$(C_6F_5N{=}CHC_6H_4O)_2$	6.5	[c]	[c]	9.2	[c]	[c]
$[CH_2N(Me)CH_2C_6H_4O]_2$	0.01	[c]	[c]	2.5	[c]	[c]

[a] See text and ref 33 for definition of "intrinsic barrier. [b] TS_B could not be located and most likely does not exist. [c] Not calculated. [d] *After ZPE correction*, the SOSP is below TS_A or TS_B, and the intrinsic barrier cannot be calculated.

effect of changing relative BHT_A/BHT_B energies from the underlying trends, we have included in Table 4 the *intrinsic* "barrier" between TS_A and TS_B, obtained by approximating the path between TS_A and TS_B via the SOSP by a two-term cosine function.[33] These intrinsic barriers seem to depend little on the metal and show only a weak dependence on the ligand structure. Their small magnitude is the underlying reason why changes in the relative energies of BHT_A and BHT_B can easily lead to qualitative changes in the PES, such as the disappearance of a whole reaction path.

The BHT_A/BHT_B area of the PES can be described using only two reaction coordinates: one measuring the degree of hydrogen transfer between the olefins and one measuring the M−H distance and the opening of the CMC angle. This allows representation as an energy contour diagram. Schematic drawings[34] representing the cases mentioned before are shown in Figure 3. The solid black lines represent normal reaction paths

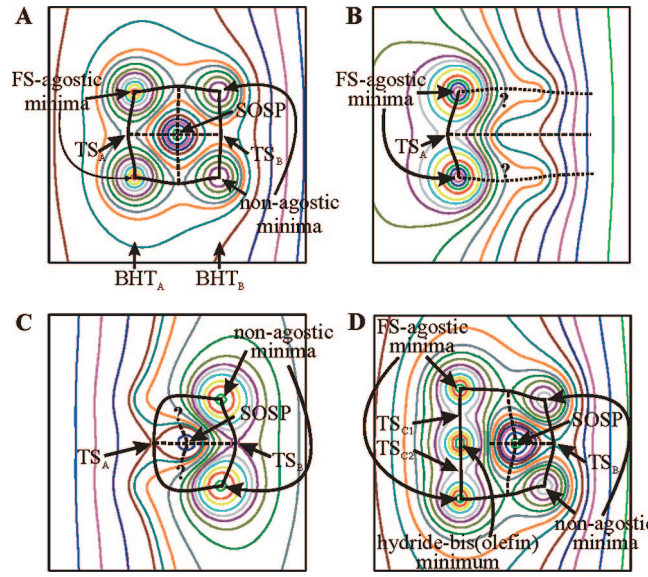

Figure 3. Schematic[34] contour-level representations of PESs for various special cases. Vertical axis: H transfer. Horizontal axis: M−H interaction/CMC opening.

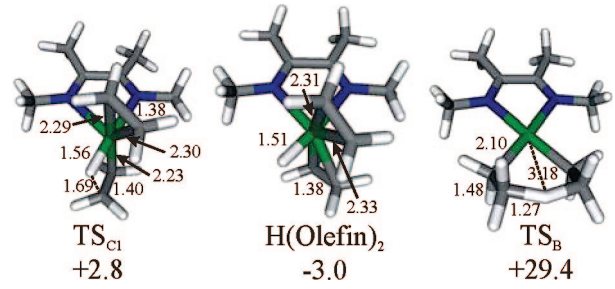

Figure 4. BHT and insertion in the α-diimine Pd^{II} model system. Bond lengths in Å, angles in deg, relative energies (ΔH^0_{0K}) in kcal/mol.

(as would, for example, be found by IRC following), while the dotted lines are the analogous lines connecting transition states to SOSPs.[35]

Figure 3A shows the "normal" four-minima−four-transition-state situation corresponding to Scheme 6, typical of most Hf systems studied here. Figure 3B shows that raising the energy of the BHT_B path leaves only a single 2-minima−1-transition-state situation (the other "reaction paths" do not go anywhere); this corresponds to some of the more open Zr systems, where BHT_B has disappeared. Figure 3C shows how the disappearance of two local minima can lead to a two-minima−two-transition-states−one-SOSP situation, which necessarily contains some valley−ridge inflection points;[36] this would be typical of systems with weakly agostic or nonagostic metal alkyls. Finally, Figure 3D represents the case of very open systems (like Cp_2La) where the BHT_A path has been replaced by the BHT_C path.

Extension to Late-Transition-Metal and Main-Group Systems. To check the relevance of alternative BHT paths for late transition metals (LTM), we investigated two simplified model systems (see Scheme 7). These were not intended to be complete models for real active species (they lack the steric

(33) The change in energy along the TS_A−SOSP−TS_B path is written as $E(x) = {}^1/_2(1-\cos \pi x)\Delta E_{rxn} + {}^1/_2(1-\cos 2\pi x)\Delta E_{intr}$, where x is 0 at TS_A and 1 at TS_B. Using the energies for the three stationary points, and requiring the first derivative to be zero at the SOSP, the system is solved for x (at the SOSP) and for ΔE_{intr}, the latter being identified as the *intrinsic* barrier. The reaction becomes barrierless if $\Delta E_{rxn} > 4\Delta E_{intr}$.

(34) Analytic functions were chosen to clearly illustrate, in a qualitative fashion, the various types of PES. They do not correspond quantitatively to any specific system studied in this work.

(35) As far as we are aware, no method currently exists that allows following the path from an SOSP to its transition states in a manner analogous to IRC following.

(36) See e.g.: (a) Quapp, W. *Theor. Chim. Acta* **1989**, *75*, 447. (b) Valtazanos, P.; Ruedenberg, K. *Theor. Chim. Acta* **1986**, *69*, 281.

Scheme 7. LTM and Main-Group-Metal Systems Studied

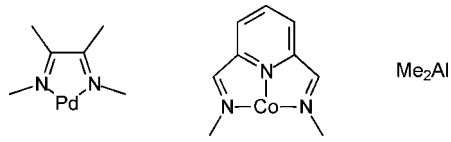

hindrance of the full systems), and only the reactivity of the $LM(Et)^+$ species with ethene was investigated.

The first system is a model for Brookhart α-diimine palladium(II) catalysts;[37] similar and more sophisticated models have been studied before by the groups of Ziegler[14] and Morokuma.[13] Relevant structures are shown in Figure 4. In agreement with Morokuma, we find that the BHT_B path exists, but is far too high in energy to compete with olefin insertion. Both insertion and BHT_B occur in the plane of the LPd fragment, as expected. In contrast, associative olefin displacement involves a five-coordinate intermediate and follows a BHT_C-like path with a discrete hydride−bis(olefin) complex; displacement occurs in a plane perpendicular to the LPd plane.[13,14] This large difference in geometries between TS_C and TS_B leads to a situation where the two paths are completely separated, without even a SOSP to connect their transition states. We expect all square-planar d^8 catalysts to follow this pattern. More bulky ligands will destabilize the BHT_C path relative to insertion, but they are not expected to affect the BHT_B/insertion ratio much.

The second LTM system studied is a diiminepyridine cobalt(II) system that is a model for Brookhart/Gibson Co catalysts;[38] this system has also been studied by the group of Ziegler.[39] Because considerable uncertainty exists about the nature of the active species and its spin state, we checked both high-spin (HS) and low-spin (LS) variations, using two different functionals (B3LYP and BP86). B3LYP produces very similar energies for HS and LS species, while at the BP86 level the LS state is much lower in energy than the HS state (by ca. 20 kcal/mol).[40]

For the LS state of the model Co catalyst, both BHT_A and BHT_B paths exist (Figure 5), but BHT_A is strongly preferred (by 14−20 kcal/mol) and is in fact calculated to be *easier* than insertion. Indeed, Ziegler argued that, like for the α-diimine catalysts, steric hindrance is essential here to prevent easy associative olefin exchange. The main difference with the Pd case is that for this Co system BHT_A and BHT_B occur in similar geometries and are connected by a SOSP only 1−2 kcal/mol above TS_B.

The HS state of the model Co catalyst presents a rather different picture. At the BP86 level, BHT_A and BHT_B are now close in energy, and the SOSP is only slightly above BHT_B. At the B3LYP level, a stronger preference for BHT_B is found, to the extent that the BHT_A path ceases to exist.

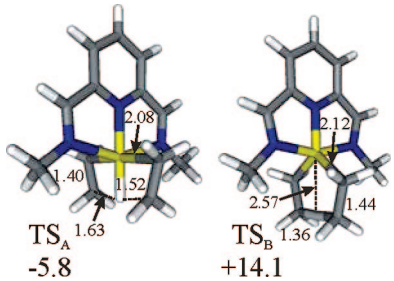

Figure 5. BHT transition states for the diiminepyridine LS−Co^{II} model system (B3LYP functional). Bond lengths in Å, energies (ΔH^0_{0K}, relative to insertion TS) in kcal/mol.

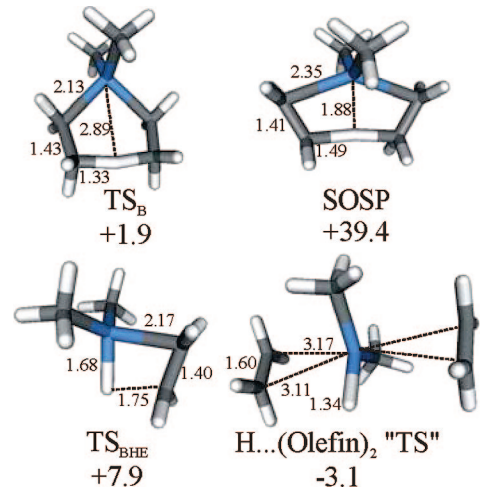

Figure 6. BHT and BHE in the Me_2Al system. Bond lengths in Å, energies (ΔH^0_{0K} relative to insertion TS) in kcal/mol.

The main conclusion to be drawn from these results for LTM model systems is that metal−alkyl−olefin complexes having an additional metal acceptor orbital (Pd^{II}, LS−Co^{II}) prefer an associative path (BHT_c or BHT_A), whereas for less unsaturated systems (HS−Co^{II}) the BHT_B path becomes competitive.

After studying the "aluminum-like" BHT_B path for transition metals, it is now useful to have a second look at Al and see whether we can recognize alternative chain-transfer paths here; we therefore revisited the Me_2AlEt/C_2H_4 system (Figure 6 shows a few relevant stationary points). The BHT_B path for this and related Al systems has been discussed extensively in previous work.[10] The main competing chain-transfer reaction is purely dissociative BHE: the binding energy of ethene to Me_2AlH is only a few kcal/mol; thus, in contrast to cationic early transition metal (ETM) catalysts, the "naked" hydride is easily accessible. We also managed to locate a transition state for associative displacement of one ethene molecule by another at Me_2AlH, but both olefins are extremely weakly bound, so this is not very different from the completely dissociative BHE path. Interestingly, we could still find an SOSP between TS_B and this weakly bound $Me_2AlH(C_2H_4)_2$ "structure", but it is very high in energy. This means that, unlike for early transition metals, the two paths are well separated and will exist independently even if the system is significantly modified. One reason for the high SOSP may be that the Al atom simply does not have enough valence orbitals available for binding both the hydride and the two olefin fragments; that would explain the large difference with transition metals of similar electronegativity.

Extension to "Hetero-olefins". In view of the generality of the two-transition-state situation for early transition olefin polymerization catalysts, we wondered whether "hetero-olefins" such as carbonyl compounds would show a similar behavior. As an example, we studied the reaction of $Cp_2TiO^iPr^+$ with acetaldehyde to give Cp_2TiOEt^+. A TS_B-like transition state could easily be located and is similar in character to those found

(37) Johnson, L. K.; Killian, C. M.; Brookhart, M. *J. Am. Chem. Soc.* **1995**, *117*, 6414.

(38) (a) Small, B. L.; Brookhart, M.; Bennett, A. M. A. *J. Am. Chem. Soc.* **1998**, *120*, 4049. (b) Britovsek, G. J. P.; Gibson, V. C.; McTavish, S. J.; Solan, G. A.; White, A. J. P.; Williams, D. J.; Kimberley, B. S.; Maddox, P. J. *Chem. Commun*. **1998**, 849.

(39) Margl, P.; Deng, L.; Ziegle, T. *Organometallics* **1999**, *18*, 5701.

(40) For the homologous Fe systems, BP86 also shows a higher preference for LS states than B3LYP; compare: (a) Deng, L.; Margl, P.; Ziegler, T. *J. Am. Chem. Soc.* **1999**, *121*, 6479. (b) Khoroshun, D. V.; Musaev, D. G.; Vreven, T.; Morokuma, K. *Organometallics* **2001**, *20*, 2007.

Table 5. Insertion and BHT for Diiminepyridine Co Model System (energies in kcal/mol relative to LS insertion TS)

functional	spin state	TS_{ins}	TS_A	TS_B	SOSP
B3LYP	HS	−1.3	[a]	8.3	[a]
	LS	(0)	−5.8	14.1	14.7
BP86	HS	15.0	28.8	27.4	32.3
	LS	(0)	−4.2	10.9	12.9

[a] TS_B and SOSP could not be located and most likely do not exist.

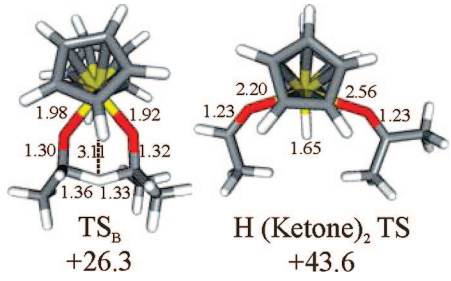

Figure 7. BHT in $Cp_2TiO^iPr^+$ + MeCHO. Bond lengths in Å, energies (ΔH^0_{0K} relative to $Cp_2TiOEt(OCMe_2)^+$) in kcal/mol.

for the all-carbon analogues (Figure 7). It corresponds to the Meerwein−Ponndorf−Verley (MPV) reduction[41] of a carbonyl compound by an alcohol, a reaction that works well with aluminum[42] but can also be catalyzed by transition metals.[43]

Location of a BHT_A-like path was more problematic. However, we located a transition state that corresponds to associative displacement of one carbonyl compound by another at a Cp_2TiH^+ center. It is much higher in energy than TS_B and, unlike the olefin case, shows no sign of any interaction of the transferring hydrogen with carbon atoms; that is, it is related to the BHT_C path. Clearly, the BHT_B path will be preferred for this and similar systems. The unfavorable energy of TS_A/TS_C corresponds to the high exothermicity of aldehyde/ketone insertion in the M−H bond: for H transfer via TS_A (or TS_C), the insertion has to be completely reversed, whereas TS_B simply exchanges one M−C bond for another without deinserting the ketone.

Interestingly, the PES does not seem to have a SOSP directly connecting TS_B with the ketone displacement TS. The system does have a region with the correct curvature, but gradients stay rather large there, and on optimization, one negative eigenvalue suddenly disappears. The surface seems to have added complexity compared to the olefin case, most likely related to rotation of the organic fragments out of the MHO_2 plane.

Relevance of the BHT_B Path. After exploring the potential-energy surfaces of many systems for the presence of BHT_A and BHT_B paths, the most important question is probably: how relevant is the BHT_B path? Are there any actual polymerization systems where BHT_B is actually the preferred chain-transfer path?

To answer this question, it is not sufficient to compare the BHT_A and BT_B transition-state energies. Table 3 clearly shows that increased steric hindrance will cause BHT_B to become preferred over BHT_A, but it is still possible that at the same time BHE, which requires even less space around the metal, becomes preferred. Indeed, experiment indicates that BHE (and β-methyl elimination, not considered here) dominates for extremely hindered systems such as $Cp^*_2ZrR^+$.[44,45] Unfortunately, putting BHE on the same energy scale as the insertion and BHT paths is not trivial. One problem is that the systems differ in molecularity, which creates problems when calculating free-energy differences (especially for solutions!).[46] Also, BHE is rather different in type and will be influenced differently by solvent and counterion, whereas the BHT_A, BHT_B, and insertion transition states are so similar that solvent and counterion effects are likely to cancel;[47] both points are confirmed by test calculations (Table S2, SI). Finally, we have noted before that the balance between BHE and BHT_A varies significantly with the choice of basis set and functional;[48] Table S4 (SI) illustrates this for the simple $Cp_2Ti^iBu^+$ + propene system. Since no gas-phase data are available for calibration, we do not know at this point what the "true" value should be.

To nevertheless get an impression of the effect of ligand variation on the importance of the various chain-transfer mechanisms, we decided to use an empirical correction to "anchor" the BHE energies to the scale for BHT and insertion. A kinetic analysis by Brintzinger[7] for the $Me_2Si(BzInd)_2Zr$ and $Me_2Si(2\text{-}MeBzInd)_2Zr$ systems (in combination with MAO and propene) indicated that for the latter, in particular, BHE and BHT occurred with comparable rates. For the relative rates of BHT and propagation, he found $k_{BHT}/k_{prop} = 1.8 \times 10^{-4}$, corresponding to a difference in free energy of activation of ca. 5.5 kcal/mol; our calculated value for the same temperature (50 °C) but then in the gas phase is 8.9 kcal/mol, in "reasonable" agreement. Brintzinger also found a ratio of k_{BHE}/k_{prop} of 1.9×10^{-4} mol/L for the same ligand. The observed relative rate of these two reactions provides an experimental free-energy difference between the two of ca. 4.8 kcal/mol,[49] as compared to our calculated value of −12.0 kcal/mol for an ideal gas-phase, counterion-free system. When we apply the difference of 16.8 kcal/mol between these two values as a correction to *all* BHE

(41) (a) Meerwein, H.; Schmidt, R. *Liebigs Ann. Chem.* **1925**, *444*, 221. (b) Verley, A. *Bull. Soc. Chim. Fr.* **1925**, *37*, 537. (c) Ponndorf, W. *Angew. Chem.* **1926**, *39*, 138.

(42) Nishide, K.; Node, M. *Chirality* **2002**, *14*, 759, and references therein.

(43) Noyori, R.; Hashiguchi, S. *Acc. Chem. Res.* **1997**, *30*, 97, and references therein.

(44) (a) Resconi, L.; Piemontesi, F.; Franciscono, G.; Abis, L.; Fiorani, T. *J. Am. Chem. Soc.* **1992**, *114*, 1025. (b) Eshuis, J. J. W.; Tan, Y. Y.; Meetsma, A.; Teuben, J. H.; Renkema, J.; Evens, G. G. *Organometallics* **1992**, *11*, 362. (c) Yang, P.; Baird, M. C. *Organometallics* **2005**, *24*, 6005.

(45) Direct β-methyl migration to a coordinated monomer, analogous to our BHT_B path, has also been proposed for propene polymerization (see: Yang, P.; Baird, M. C. *Organometallics* **2005**, *24*, 6013). However, our theoretical findings do not support this hypothesis: the calculated transition state for such a process is ca. 53 kcal/mol above the insertion transition state for both the Cp_2Zr and the Cp^*_2Zr system (see Supporting Information for raw energies).

(46) For the gas-phase species, considering *free energies*, the highest point on the propagation path is the insertion TS, while the highest point on the BHE path can be either the naked metal hydride (plus one molecule each of isobutene and propene) or the BHE TS (plus one molecule of propene), depending on the system. The entropy contribution to this one vs two/three particle comparison is large and dominant, but is clearly unrealistic for solution-phase chemistry. Comparison of propagation, BHT_A, and BHT_B among each other does not suffer from this problem since these species all have the same composition.

(47) Solvent effects tend to be large in magnitude but not very differentiating between similar species. See e.g.: (a) Motta, A.; Fragalà, I. L.; Marks, T. J. *J. Am. Chem. Soc.* **2007**, *129*, 7327. (b) Borrelli, M.; Busico, V.; Cipullo, R.; Ronca, S.; Budzelaar, P. H. M. *Macromolecules* **2002**, *35*, 2835.

(48) Talarico, G.; Blok, A. N. J.; Woo, T. K.; Cavallo, L. *Organometallics* **2002**, *21*, 4939.

(49) The rate constant ratio of 1.9×10^{-4} mol/L corresponds to a ΔG_{323K} of $RT \ln 1.9 \times 10^{-4} = 5.5$ kcal/mol at [propene] = 1 mol/L. Under these conditions, $p_{propene}$ is 3 bar, and dissolved and gaseous propene are in equilibrium, so ΔG^0_{323K} referred to gaseous propene is $(5.5 - RT \ln 3) = 4.8$ kcal/mol.

(50) Using the same correction should be reasonable for other relatively crowded systems, but much less so for open systems such as Me_2CCp_2Zr. For very open systems, however, BHE could never compete anyway, so the precise value of the correction is not very relevant there.

Table 6. Estimated Relative Free-Energy Barriers (298 K, solution, 1 bar propene) for BHT_A, BHT_B, and BHE Paths Relative to Insertion[a]

	$\Delta\Delta G^0_{298.15K}$ (kcal/mol)								
	Ti			Zr			Hf		
system	BHT_A	BHT_B	BHE[a]	BHT_A	BHT_B	BHE[a]	BHT_A	BHT_B	BHE[a]
(Cp*)(EtNCMeN^{t}Bu)	20.3	8.9	−8.2	20.9	9.1	−2.0	21.9	5.7	−2.9
Cp^*_2	23.0	11.8	−3.4	15.0	12.1	3.4	15.1	8.2	3.4
Cp_2	15.2	14.2	−0.2	6.1	12.6	8.2	7.8	8.9	8.1
$Me_2Si(2\text{-}MeBzInd)_2$	17.7	15.7	3.3	8.9	12.6	6.0	10.0	8.5	6.5
$Me_2Si(BzInd)_2$	16.2	15.4	4.3	7.5	12.4	6.2	8.8	8.8	6.6
$Cp^*CH_2CH_2N^tBu$	11.2	12.0	8.2	2.1	[c]	9.4	2.0	4.0	9.4
Me_2SiCp_2	14.0	15.9	1.4	3.9	11.9	10.6	5.5	8.6	10.3
$Cp^*SiMe_2N^tBu$	10.0	11.4	10.3	1.4	[c]	10.0	1.5	4.1	11.0
Me_2CCp_2	12.1	15.8	6.9	2.1	[c]	12.2	4.2	8.2	13.3
$(C_6F_5N{=}CHC_6H_4O)_2$	11.5	14.4	−5.5[b]	[d]	[d]	[d]	[d]	[d]	[d]
$[CH_2N(Me)CH_2C_6H_4O]_2$	8.6	17.5	9.8	[d]	[d]	[d]	[d]	[d]	[d]

[a] The *highest* of TS_{BHE} and MH is used to calculate the BHE barrier, and this is adjusted by an empirical correction of 16.8 kcal/mol as explained in the text. [b] The BHE TS could not be located and most likely does not exist; insertion of isobutene in the metal hydride appears to be barrierless. [c] TS_B could not be located and most likely does not exist. [d] Not calculated.

Scheme 8. Dependence of Preferred Chain-Transfer Path on Metal Environment (only half of each chain transfer reaction is shown)

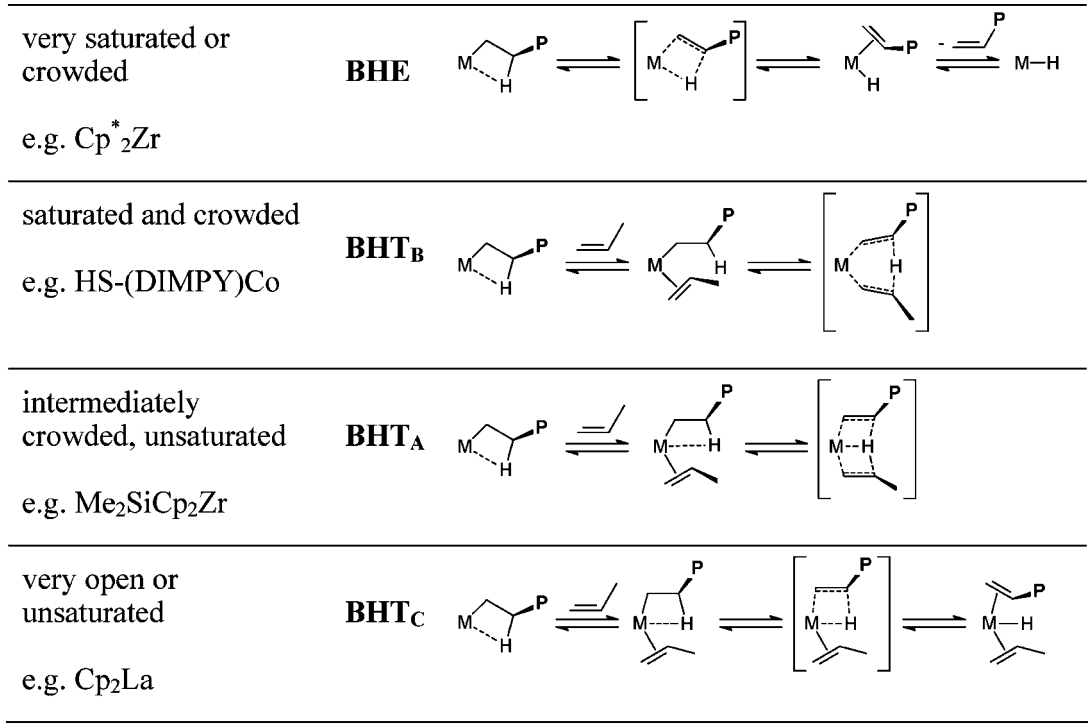

free energies,[50,51] we obtain the relative free energies listed in Table 6. We emphasize that this correction is rather crude and is likely to have an error margin of 5 kcal/mol or more, in particular for nonmetallocene systems. Unfortunately, not enough experimental data are available to allow a more reliable calibration.

As far as we know, ours is the first attempt to put calculated BHE energies on the same free-energy scale as propagation and BHT. Obviously, the validity of the comparison depends crucially on the empirical correction term used. However, the results mostly appear to be reasonable. BHE is predicted to be the dominant chain-transfer mechanism for the crowded Cp^*_2 and (Cp*)(acetamidinate) Zr/Hf systems. Experimentally, (Cp*)(acetamidinate)Zr systems give low molecular weights through dominant BHE.[52] Cp^*_2Zr and Cp^*_2Hf systems give only oligomers with propene through dominant β-Me elimination (not considered in this work), but for oligomerization of 1-butene the dominant chain-transfer mechanism is BHE.[44a] The less crowded Cp_2Zr[4d] system has been found to have dominant BHT chain transfer, with relatively low molecular weight; the MW obtained with Me_2SiCp_2Zr[53] and $Cp^*SiMe_2N^tBuZr$[54] catalysts is also relatively low. The predictions for Ti appear to overestimate the ease of BHE somewhat: Cp_2Ti polymerization is dominated by BHE, but can produce high molecular weights, be it at very low temperature.[55] The low predicted value of −5.5 kcal/mol for BHE at $(C_6F_5N{=}CHC_6H_4O)_2Ti$ is not compatible with the high MW obtainable with FI catalysts,[31] although the

(51) The use of the same free-energy correction at 25 °C as at 50 °C corresponds to a fully enthalpic correction. If the correction were fully entropic, it would be 15.5 kcal/mol (instead of 16.8) at 25 °C. In view of the crudeness of our empirical correction this difference should be irrelevant.

(52) Busico, V.; Carbonniere, P.; Cipullo, R.; Pellecchia, R.; Severn, J. R.; Talarico, G. *Macromol. Rapid Commun.* **2007**, *28*, 1128.
(53) Kaminsky, W. *Macromol. Chem. Phys.* **1996**, *197*, 3907.
(54) Jia, L.; Yang, X.; Stern, C. L.; Marks, T. J. *Organometallics* **1997**, *16*, 842.
(55) Ewen, J. A. *J. Am. Chem. Soc.* **1984**, *106*, 6355.

lack of steric hindrance at the phenol moiety of our model system might be a factor here. High molecular weights are correctly predicted for $Cp^*SiMe_2N^tBuTi$[56] and $Cp^*CH_2CH_2$-N^tBuTi[57] systems.

Returning now to the BHT_B path, our results indicate that it would only become competitive in situations of intermediate crowding, specifically for Hf. For highly crowded systems BHE dominates, and for open systems BHT_A is easier. Also, for Zr and Ti BHT_B is always so far above propagation that it is unlikely to ever become the dominant chain-transfer mechanism. Unfortunately, it would already be hard to distinguish between the BHT_A and BHT_B paths experimentally, and even harder to separate their contributions when both occur simultaneously.

Conclusions

A systematic investigation of chain-transfer paths for a variety of polymerization catalysts has revealed a range of mechanistic variations, which seem to be connected in a near-continuous way, much like the range of mechanisms recently identified for C−H bond activation reactions.[58] The controlling factor seems to be the accessibility of the metal atom, although a few other issues have been identified; Scheme 8 summarizes these findings. For ETM systems, steric factors seem to dominate the outcome; for LTM systems, details of the specific system (electron count, spin state) are also relevant, and it is hard to draw general conclusions.

One remarkable aspect of this mechanistic diversity is the independent existence, for many systems, of BHT_A and BHT_B paths, and the rather low energy separation between them. BHT_B is not expected to be the dominant chain-transfer mechanism for many ETM polymerization catalysts, but might be relevant for some Hf systems of intermediate crowdedness. The BHT_B path should be more relevant for main-group-metal systems such as alkylaluminums. For "hetero-olefin" derivatives (alkoxides, amides) of electropositive metals, where deinsertion to the hydride-like TS_A is too much uphill, the BHT_B path should always be preferred, to the extent that often the BHT_A path will not exist; this is relevant to, for example, alkoxide-to-ketone hydride transfer (MPV reduction).

Location of second-order saddle points connecting TS_A and TS_B has been helpful in understanding changes in the PES on ligand variation. The PES is seen to be rather flat near the chain-transfer transition states, and moving toward more open ETM systems can result in a complete disappearance of TS_B and the SOSP. This flatness of the PES, which translates in high flexibility of BHT TS geometries, may be one of the reasons why it is so hard to control the molecular weight produced by a polymerization catalyst using rational ligand design.

Acknowledgment. G.T. acknowledges a contribution from the Italian Ministry for University (PRIN 2006) and the Centro di Metodologie Chimico-Fisiche (CIMCF), University of Naples "Federico II", for computer time. P.H.M.B. is grateful for financial support from Sabic Europe, the Province of Manitoba, and the Canada Foundation for Innovation for grants to set up a computational facility.

Supporting Information Available: Tables of total energies, for all systems studied, at various levels of theory. Thermal corrections and lowest six non-null frequencies for all systems. Spreadsheet containing all raw energies and data for Tables 1−9. Movie files illustrating imaginary-frequency normal modes for transition states and second-order saddle points for the Cp_2Ti and $Me_2Si(2\text{-}MeBzInd)_2Hf$ systems. Full citation for Gaussian03 (ref 19). Zipped archive of *xyz*-format coordinates files. This material is available free of charge via the Internet at http://pubs.acs.org.

OM800313N

(56) McKnight, A. L.; Waymouth, R. M. *Chem. Rev.* **1998**, *98*, 2587.
(57) Sinnema, P.-J.; Hessen, B.; Teuben, J. H. *Macromol. Rapid Commun.* **2000**, *21*, 562.
(58) Vastine, B. A.; Hall, M. B. *J. Am. Chem. Soc.* **2007**, *129*, 12068.